

NASA TECHNICAL
MEMORANDUM

N74-11335
NASA TM X-62,314

NASA TM X-62,314

AQUEOUS CHLORIDE STRESS CORROSION CRACKING OF TITANIUM - A
COMPARISON WITH ENVIRONMENTAL HYDROGEN EMBRITTLEMENT

Howard G. Nelson

Ames Research Center
Moffett Field, Calif. 94035

FACILITY FORM 602	<u>N74-11335</u> (ACCESSION NUMBER)	<u> </u> (THRU)
	<u>30</u> (PAGES)	<u>G3</u> (CODE)
	<u>TMX62314</u> (NASA CR OR TMX OR AD NUMBER)	<u>17</u> (CATEGORY)

September 1973

AQUEOUS CHLORIDE STRESS CORROSION CRACKING OF TITANIUM -
A COMPARISON WITH ENVIRONMENTAL HYDROGEN EMBRITTLEMENT

Howard G. Nelson

Ames Research Center, NASA
Moffett Field, California 94035

ABSTRACT

The physical characteristics of stress corrosion cracking of titanium in an aqueous chloride environment are compared with those of embrittlement of titanium by a gaseous hydrogen environment in an effort to help contribute to the understanding of the possible role of hydrogen in the complex stress corrosion cracking process. Based on previous studies, the two forms of embrittlement are shown to be similar at low hydrogen pressures (100 N/m^2) but dissimilar at higher hydrogen pressures. In an effort to quantify this comparison, tests were conducted in an aqueous chloride solution using the same material and test techniques as had previously been employed in a gaseous hydrogen environment. The results of these tests strongly support models based on hydrogen as the embrittling species in an aqueous chloride environment. Further, it is shown that if hydrogen is the causal species, the effective hydrogen fugacity at the surface of titanium exposed to an aqueous chloride environment is equivalent to a molecular hydrogen pressure of approximately 10 N/m^2 .

INTRODUCTION

Stress-corrosion cracking, of a metal in general and of titanium in particular, is a complex process dependent on both metallurgical and environmental variables. As an example, for titanium alloys, aqueous chloride solutions (salt water solution containing 3.5% NaCl) have been observed to affect some alloys while others are apparently immune from attack.¹ Additionally, some alloys are immune from attack by molten MgCl_2 , but are deleteriously affected by aqueous chloride solutions.² The results of these and numerous other studies³⁻⁵ have produced an extensive debate as to the causal species involved in the stress corrosion cracking of titanium alloys. Under seemingly identical environmental conditions, stress-corrosion cracking has been explained both by a hydrogen embrittlement mechanism^{4,6} as well as by a stress-sorption mechanism involving a halide ion.⁷ In fact, resolution of the role of hydrogen in the stress-corrosion cracking of titanium alloys has been identified by some⁸ as the major barrier to the understanding of the stress-corrosion cracking process.

A simple high purity gaseous hydrogen environment has been shown to have a deleterious effect on the fracture behavior of many metals⁹ including titanium.¹⁰⁻¹² This form of embrittlement invites comparison with stress corrosion in that, a hydrogen, a potential causal species in aqueous chloride stress corrosion, is isolated from the much more complex aqueous chloride environment. Although one involves a gaseous environment and the other a liquid environment, both forms of embrittlement are

inherently similar in that the embrittling species is not originally present within the metal but must interact with or enter through the metal surface while the metal is in a state of stress.

It is the purpose of the present paper to compare environmental hydrogen embrittlement and aqueous chloride stress corrosion cracking of titanium in an effort to help contribute to the understanding of the role of hydrogen in the complex stress corrosion process. First, environmental hydrogen embrittlement of α - β titanium will be considered in terms of the results of recent investigations¹⁰⁻¹² in order that the physical manifestations of this form of embrittlement can be catalogued. The interpretation of these results will be summarized in an effort to better understand the mechanistic aspects of this form of embrittlement. Next, the discussion will be extended to include observations made by other investigators on the stress corrosion cracking of titanium alloys in aqueous chloride solutions in which hydrogen may play a role in the cracking process. The physical characteristics of stress corrosion cracking will be qualitatively compared with those of environmental hydrogen embrittlement. Finally, in an effort to quantify this comparison, the results of the present investigation, conducted in an aqueous chloride environment using the same material and similar test technique as previously employed in the gaseous hydrogen studies¹⁰⁻¹² will be presented and discussed.

GASEOUS HYDROGEN EMBRITTLEMENT OF TITANIUM

Environmental hydrogen embrittlement of the Ti-6Al-4V alloy was first investigated as a function of variations in alloy microstructure and test displacement rate at a hydrogen pressure of near one atmosphere 90.6 K N/m^2 (680 torr) at room temperature.¹⁰ All microstructures studied were found to be susceptible to environmental hydrogen embrittlement; however, the degree of susceptibility was observed to be strongly dependent on both test displacement rate and microstructure. For a given microstructure, embrittlement was found to increase with decreasing test displacement rate, as shown in Fig. 1. Plotted in this figure is the ratio K_{scg}/K_Q , a measure of embrittlement, versus displacement rate where K_{scg} is a nonstandard stress-intensity for the initiation of measurable subcritical crack growth and K_Q is a non-valid critical stress intensity for failure. As seen in Fig. 1, for any given test displacement rate, at a constant hydrogen pressure of 90.4 kN/m^2 , the microstructure described as equiaxed α was found to be the less embrittled while the microstructure described as acicular α in a β matrix was found to be the more embrittled.

When the Ti-6Al-4V alloy having microstructures of acicular α and equiaxed α were investigated as a function of hydrogen pressure¹², embrittlement of the microstructures was found to exhibit strikingly different pressure dependencies as shown in Fig. 2. It is seen from this figure that for a fixed displacement rate, hydrogen at a pressure near 1 atm ($9.04 \times 10^4 \text{ N/m}^2$) embrittles both structures, but has a greater effect on the alloy having a continuous β -matrix (acicular α in a β matrix) than on that with a continuous α -matrix (equiaxed α).

As the hydrogen pressure is decreased, however, the degree of embrittlement observed in the specimens having a continuous β -matrix decreases until, at a hydrogen pressure of approximately 1 N/m^2 , no embrittlement is observed. In contrast to these observations, in specimens with a continuous α -matrix, the degree of embrittlement appears to be unaffected by a decrease in the environmental hydrogen pressure down to at least 1.3 N/m^2 , the lowest pressure of the study.

The microscopic fracture path of hydrogen-induced slow crack growth was also examined.¹² In specimens having a continuous α -matrix, growth at all pressures investigated appears to be primarily transgranular through the α -phase grains accompanied by a minor amount of intergranular growth. In specimens having a continuous β -matrix, a change in hydrogen pressure was observed to affect the predominant microscopic fracture path. Figs. 3(a) and 3(b) are photomicrographs of typical subsurface cracks observed in specimens having a continuous β -matrix and fractured in hydrogen at $9.06 \times 10^4 \text{ N/m}^2$ (Fig. 3(a)) and at $1.3 \times 10^1 \text{ N/m}^2$ (Fig. 3(b)). It is seen that at the higher hydrogen pressure, the predominant form of cracking occurs in an intergranular manner along prior β and transformed α platelet boundaries, however, at the lower hydrogen pressure, cracking is primarily transgranular through the prior β grains and across the transformed α platelets.

Specimen profiles comparing macroscopic, hydrogen-induced, slow crack growth patterns observed in specimens having the two microstructures are shown in Fig. 4. Hydrogen-induced slow crack growth in the acicular

microstructure (Fig. 4(a)) is seen to occur with little or no crack branching and the macroscopic crack growth direction is essentially normal to the maximum applied load at all hydrogen pressures studied. In the equiaxed α microstructure (Fig. 4(b)), however, hydrogen-induced slow crack growth results in severe crack branching away from the normal crack growth direction at all environmental hydrogen pressures studied.

The above observations of environmental hydrogen embrittlement of Ti-6Al-4V alloy are summarized in Table I. In this table, the first column lists the characteristics on which the observations are based, the second column lists the conditions placed on the observations, and the third and fourth columns list the observations made on specimens having microstructures of a continuous α -phase with dispersed β in the boundaries, and of a continuous, β -phase surrounding the α -phase titanium, respectively. Based on these results, it was suggested¹⁰⁻¹² that environmental hydrogen embrittlement of α - β titanium is controlled by the rate processes involved in the competition of intergranular cracking along α/β boundaries and transgranular cracking across α grains.

It is hypothesized that when a continuous network of β phase is present in the microstructure, a "short-circuit" transport path exists which enables hydrogen to penetrate more readily into the titanium lattice. Here, the rate process exhibits an apparent activation energy of 23.0 MJ/mole (5500 cal/mole) and appears to be bulk diffusion of hydrogen through β -phase titanium.¹¹ As the hydrogen pressure is decreased, the solid-solution hydrogen concentration in the β phase near the crack tip surface

TABLE I. - PHYSICAL MANIFESTATIONS OF ENVIRONMENTAL HYDROGEN
EMBRITTLMENT OF Ti-6Al-4V ALLOY

Characteristic	Conditions	Observations	
		Continuous α microstructure (equiaxed α)	Continuous β microstructure (acicular α)
Time dependence	Moderately fast to moderately slow displacement rates, D	Embrittlement increases with decreasing rate	Embrittlement increases with decreasing rate
	9.04×10^4 N/m ² P _{H₂} at moderately slow D	Moderate embrittlement	Severe embrittlement
	100 N/m ² P _{H₂} at moderately slow D	Moderate embrittlement	Moderate embrittlement
Hydrogen pres- sure dependence	1 N/m ² P _{H₂} at moderately slow D	Moderate embrittlement	Negligible embrittlement
	All pressures and displacement rates	Severe	Negligible
Hydrogen-induced crack branching	9.04x10 ⁴ N/m ² P _{H₂}	Transgranular cleavage	Intergranular
	100 N/m ² P _{H₂}	Transgranular cleavage	Transgranular cleavage
	1 N/m ² P _{H₂}	Transgranular cleavage	None

is lowered through the normal equilibrium relations, the concentration-gradient induced hydrogen transport in the β phase is decreased, less hydrogen is able to penetrate into the microstructure in a given time period, and embrittlement is decreased (Fig. 2). In microstructures containing a continuous matrix of α phase, the short-circuit hydrogen transport path does not exist. Hydrogen must, then, interact directly with α -phase titanium initially forming a thin, continuous hydride layer on the clean α titanium surface. Under such conditions, further hydride growth will be diffusion limited in a manner similar to that described by the Wagner theory of oxidation.¹³ Under the conditions of the present study, where the hydrogen pressure is much greater than the hydride dissociation pressure,^{14,15} further hydride growth will be nearly independent of hydrogen pressure.¹³ Additionally, transgranular cracking observed in this microstructure is consistent with the idea of hydride formation^{16,17} within the α -phase titanium grains.

The change in fracture path in the acicular microstructure (continuous β -phase), observed to result from variations in hydrogen pressure (Fig. 3), is consistent with the idea of competing processes. At higher pressures, intergranular cracking dominates because hydrogen can be readily transported in the β phase and can interact with the α phase at the boundaries in a manner similar to that proposed by Craighead et al.¹⁸ At low pressures, however, equilibrium solubility decreases and hydrogen transport is no longer enhanced in the β phase. In fact, embrittlement will be less than that observed in a continuous α matrix microstructure because cracks propagating through the α phase are blunted by the β phase at the boundaries.

A COMPARISON BETWEEN STRESS-CORROSION
CRACKING AND ENVIRONMENTAL HYDROGEN EMBRITTLEMENT

Both aqueous chloride stress corrosion cracking and environmental hydrogen embrittlement have inherent similarities in that an interaction between the environment and the metal must take place during the embrittlement process. Such similarities are implied in all forms of environmental embrittlement and will not be dwelt upon here, but include the need for local removal of the protective oxide film normally present on the metal surface (either by deformation or dissolution),¹⁹ and the maintenance of this contaminant-free metal surface by an environment free of passivators, such as an oxygen contaminant in a gaseous hydrogen environment.²⁰

Stress corrosion cracking of titanium alloys in aqueous chloride solutions has been studied extensively and several good reviews are available.³⁻⁵ Table II is a summary of some of the physical characteristics of this form of stress-corrosion cracking. These characteristics can now be compared with similar observations made in a gaseous hydrogen environment (Table I).

Stress corrosion cracking of titanium alloys is a time dependent phenomenon (Table II), indicating that embrittlement is controlled by a rate process. Boyd²² has recently studied the kinetics of crack growth in the Ti-8Al-1Mo-1V alloy having an equiaxed α structure and concludes that crack growth rate is controlled by the rate of production or by the diffusion of some embrittling species. The apparent activation energy for crack growth was observed to be 23.4 MJ/mole (5600 cal/mole). These rate kinetics are at the least qualitatively similar to those observed in environmental

TABLE II. - PHYSICAL MANIFESTATIONS OF AQUEOUS CHLORIDE
STRESS-CORROSION CRACKING OF TITANIUM

Characteristic	Observations	
	Continuous α microstructure (equiaxed α)	Continuous β microstructure (acicular α)
Time dependence	Time to failure in- creases as static load decreases	Time to failure in- creases as static load decreases
Susceptibility	Severe	Moderate to negligible
Aqueous chloride- induced crack branching	Severe	No data
Aqueous chloride- induced fracture mode	Transgranular cleavage	Transgranular cleavage

hydrogen embrittlement where the degree of embrittlement was found to be inversely dependent on the test displacement rate (Table I). Additionally, it is interesting to note that the apparent activation energy observed for crack growth in a hydrogen environment¹¹ (23.0 MJ/mole) is nearly identical to that observed in an aqueous chloride environment.

Microstructure plays a primary role in determining the susceptibility of titanium alloys to stress corrosion (Table II). Lane, et al, has studied a large number of titanium alloys having a variety of microstructures exposed to a seawater environment. In general, they conclude that the α -phase alloys are the most susceptible and that treatments which produce a continuous β -phase microstructure lessen and many times eliminate the susceptibility of the alloy to stress-corrosion cracking. This conclusion is further supported by more recent studies.²³⁻²⁷ Specifically, considering the Ti-6Al-4V alloy, Curtis and Spurr²⁶ found that the equiaxed α -phase microstructures are susceptible to stress-corrosion cracking and that treatments which transform this structure to an acicular morphology lessen susceptibility. In a comparison of these observations with those of environmental hydrogen embrittlement (Table I), it is seen that a similarity exists only at low hydrogen pressures - less than 100 N/m² (8×10^{-1} torr) (Fig. 2). At the higher hydrogen pressures, the microstructural dependence is the reverse for these two forms of embrittlement.

The macroscopic fracture path, microscopic fracture path, and fracture mode all are affected by an aqueous chloride environment (Table II). In structures with primarily α -phase titanium, stress-corrosion cracking in

general is associated with severe macroscopic crack branching,²⁷ with transgranular cracking of the α -phase grains,^{23,24,26} and with a mode of failure described as cleavage,^{26,28,29} quasi-cleavage,³⁰ or nonclassical cleavage.³¹ Consistent with these observations, environmental hydrogen embrittlement of the Ti-6Al-4V alloy having a similar continuous α -phase microstructure is associated with severe crack branching (Fig. 4(b)), primarily transgranular failure with both transgranular and intergranular subsurface cracking, and the failure mode described as nonclassical cleavage (Table I). In structures with primarily coarse, acicular α -phase titanium, Lane, et al.,²¹ has observed that in seawater, stress-corrosion cracking occurred transgranularly through prior β grains and across the transformed α platelets. These observations are in agreement with the hydrogen-induced crack path observed at the intermediate hydrogen pressure of 13 N/m² (1×10^{-1} torr) (Fig. 3(b)). Again, at higher hydrogen pressures, this similarity does not exist (Fig. 3(a)).

In summary, some of the physical characteristics of stress-corrosion cracking of titanium in an aqueous chloride environment have been qualitatively compared with those of environmental hydrogen embrittlement of titanium. At hydrogen pressures near one atmosphere, only a few obvious similarities exist between these two forms of embrittlement. However, at hydrogen pressures of less than 100 N/m² (8×10^{-1} torr), a qualitative similarity has been shown to exist. At these lower hydrogen pressures, both forms of embrittlement exhibit (1) a time dependent failure indicating the occurrence of a rate process, (2) a similar microstructural sensitivity with embrittlement most severe in microstructures having a

continuous α -phase matrix, and (3) embrittlement associated with severe crack branching and a transgranular cleavage mode of failure. Although the role of hydrogen in the aqueous chloride stress-corrosion cracking of titanium cannot be ascertained from this comparative study, it has been established that under a particular set of conditions (low environmental hydrogen pressures), the two forms of embrittlement are similar.

EXPERIMENTS AND DISCUSSION

Tests were conducted on Ti-6Al-4V in a 3.5% NaCl aqueous environment using the same material and similar test technique as previously employed in the gaseous hydrogen studies.^{10,12} This was done in order to make a direct comparison of these two forms of embrittlement.

The material was commercially obtained Ti-6Al-4V alloy, received in the mill-annealed condition. Prior to testing, all specimens were given one of the following two heat treatments: (1) solution treated at 1103°K for 40 min, water quenched, and aged at 783°K for 12 hr; or (2) solution treated at 1311°K for 40 min, stabilized at 977°K for 1 hr and 866°K for 1 hr, and air cooled. All heat treating was done in a vacuum furnace. For that heat treatment requiring rapid quench rate, the furnace was back-filled with argon immediately before quenching (while the specimen was kept at temperature) and then the specimen was removed and quenched in less than 2 sec.

The microstructures resulting from the two heat treatments are shown in Fig. 5 and are identical to those of the previous study.¹² As can be seen, the low-temperature solution treatment and age (Fig. 5(a)) resulted in primary α -phase, equiaxed grains forming a continuous matrix with the retained β -phase finely dispersed in the α boundaries. The solution treatment, done at temperatures well into the β -field and followed by a stabilization (Fig. 5(b)), resulted in a structure of coarse, acicular α -phase transformed α needles in a β matrix.

Fracture tests were conducted using the same specimen configuration and loading mode as previously employed.¹² Specimens were precracked bend specimens which were loaded in three-point bending. These specimens did not conform to the ASTM thickness guideline for plane-strain fracture toughness specimens but, since the data to be obtained were intended to be only comparative in nature, this was considered to be relatively unimportant. Stress intensity values were calculated from the maximum load measured on the load-displacement record by using a fourth-degree polynomial expression for pure bending.³² As in the previous tests, these nonstandard stress intensity values are designated as K_{scg} , the stress-intensity for the initiation of measurable subcritical crack growth.

All tests were conducted at room temperature and at a constant displacement rate, \dot{D} , of 8.9×10^{-8} m/sec in an environment of 3.5% NaCl by weight in distilled water. The solution was contained in a lucite vessel and all metallic components exposed to the solution, with the exception of the test specimen, were isolated by the use of a continuous polymeric

coating. The solution had a pH of approximately 6 and tests were conducted under conditions of uncontrolled potential.

Five tests were conducted under identical conditions on specimens having each of the two microstructures (Fig. 5). The results of these tests are summarized in Table III as the ratio K_{scg}/K_Q . Also shown in this table are the mean and standard deviation for the two sets of data. As is seen, specimens of both microstructures were influenced by the aqueous chloride environment with the equiaxed microstructure (continuous α -phase) more severely affected than the acicular microstructure (continuous β -phase) specimens. These results are consistent with the microstructure dependence of aqueous chloride stress corrosion cracking observed in Ti-6Al-4V as previously reported by Curtis and Spurr²⁶ and are consistent with that observed in a gaseous hydrogen environment only at hydrogen pressures less than 100 N/m^2 (8×10^{-1} torr) (Fig. 2).

The data of the present study (Table III), obtained in an aqueous chloride solution, are directly compared with similar data obtained in a gaseous hydrogen environment¹² in Fig. 6. This figure, a replot of Fig. 2, shows embrittlement as a function of hydrogen pressure for the two microstructures tested. Superimposed on this figure are two horizontal dashed lines indicating the degree of embrittlement observed in an aqueous chloride environment for the two microstructures tested under otherwise identical conditions. As seen in Fig. 6, severity of embrittlement is nearly identical in specimens having an equiaxed microstructure (Fig. 5(a)) in either environment. Since gaseous hydrogen embrittlement of this microstructure

TABLE III. - SUMMARY OF RESULTS OF THREE-POINT BEND
TESTS CONDUCTED IN A 3.5% NaCl AQUEOUS
SOLUTION

K_{scg}/K_Q	
continuous α microstructure (equiaxed α)	continuous β microstructure (acicular β)
0.80	0.84
0.70	0.88
0.87	0.98
0.73	0.84
0.80	0.87
<hr/>	<hr/>
mean 0.78	mean 0.88
Standard deviation from mean = 0.07	Standard deviation from mean = 0.06

is seemingly independent of hydrogen pressure yet results from the presence of the hydrogen species, the similarity in the ratio K_{scg}/K_Q observed in the two environments is strong evidence that hydrogen is the causal species in the aqueous chloride environment. This is further substantiated by the nearly identical fracture appearance of specimens failed in the two environments, as seen in Fig. 7. This figure consists of SEM fractographs of equiaxed titanium specimens failed in hydrogen (Fig. 7(a)) and in aqueous chloride (Fig. 7(b)) environments. As seen in this figure, both fracture surfaces contain numerous subsurface cracks which appear to be both intergranular and transgranular. Additionally, both surfaces contain faint wavy striations.

If hydrogen is the species which embrittles titanium in an aqueous chloride environment, the environmental influence on specimens having an acicular microstructure dictates that in aqueous chloride the effective hydrogen fugacity at the titanium surface must be equivalent to a molecular hydrogen pressure of less than 100 N/m^2 (8×10^{-1} torr). This is better seen in Fig. 6. For the material and conditions of the present tests, the effective equivalent hydrogen pressure must be approximately 10 N/m^2 (8×10^{-2} torr) — the pressure of a hydrogen environment where the severity of embrittlement is observed to be equal to that noted in the aqueous chloride environment.

The fracture appearance of acicular specimens failed in an aqueous chloride environment also substantiates the idea of hydrogen being present at the titanium surface at low concentrations. Figure 8 is a SEM

fractograph of an acicular titanium specimen failed in an aqueous chloride environment. As seen from this figure, failure occurred by a combination of transgranular failure and ductile tearing, is similar to that observed in a molecular hydrogen environment at less than 100 N/m^2 (8×10^{-1} torr) and is much different than that observed at high hydrogen pressures.¹²

SUMMARY

The physical characteristics of gaseous hydrogen embrittlement of α - β titanium have been compared with those of stress corrosion cracking of titanium in an aqueous chloride environment. From previous data it was seen that only a few obvious similarities exist between these two forms of embrittlement at high hydrogen pressures (near one atmosphere). However, at hydrogen pressures of less than 100 N/m^2 (8×10^{-1} torr), a qualitative similarity does seem to exist. Both forms of embrittlement exhibit (1) a similar time dependent failure indicating the occurrence of the same rate process, (2) a similar microstructural sensitivity with embrittlement most severe in microstructures having an equiaxed α -phase matrix, and (3) embrittlement associated with severe crack branching and a transgranular cleavage mode of failure.

In an effort to help quantify the comparison between the two forms of embrittlement, tests were conducted in an aqueous chloride solution using the same material and test techniques as had previously been employed in a gaseous hydrogen environment. For specimens having an equiaxed microstructure, severity of embrittlement and mode of failure were found to be nearly

identical in both environments. This similarity strongly supports the premise that hydrogen is the embrittling species in an aqueous chloride environment as well. If hydrogen is in fact the causal species, from a comparison of the environmental influence on specimens having an acicular microstructure, it is dictated that the effective hydrogen fugacity at the titanium surface must be equivalent to a molecular hydrogen pressure of approximately 10 N/m^2 (8×10^{-2} torr).

REFERENCES

1. I. R. Lane, Jr., O. L. Cavallaro, and A.G.S. Morton: "Fracture Behavior of Titanium in the Marine Environment." 1965, U. S. Navy MEL Report 231/65.
2. M. G. Fonatana: Ind. and Eng. Chem., 1956, Vol. 48, p. 9.
3. W. K. Boyd: "Fundamental Aspects of Stress-Corrosion Cracking." 1969 (ed. R. W. Staehle), NACE (Houston), p. 593.
4. E. L. Owen, F. H. Beck and M. G. Fontana: "Stress Corrosion Cracking of Titanium Alloys." 1970, Research Foundation, Ohio State University, Report 8, RF Project 2267, Columbus, Ohio.
5. T. R. Beck, M. J. Blackburn, and W. H. Smyrl: "Fundamental Investigation of Stress Corrosion Cracking." 1972, Boeing Company, Document D180-15006-1, Seattle, Washington.
6. G. Sanders, D. T. Powell, and J. C. Scully: "Fundamental Aspects of Stress-Corrosion Cracking." 1969 (ed. R. W. Staehle), NACE (Houston), p. 638.
7. T. R. Beck: "Fundamental Aspects of Stress-Corrosion Cracking." 1969 (ed. R. W. Staehle), NACE (Houston), p. 605.
8. S. P. Rideout and J. C. Scully: "Fundamental Aspects of Stress-Corrosion Cracking." 1969 (ed. R. W. Staehle), NACE (Houston), p. 591.
9. R. J. Walter and W. T. Chandler: Rocketdyne Research Report, 1969, R-7780-1.
10. H. G. Nelson, D. P. Williams, and J. E. Stein: Met. Trans., 1972, Vol. 3, pp. 469-475.
11. D. P. Williams and H. G. Nelson: Met. Trans., 1972, Vol. 3, pp. 2107-2113.
12. H. G. Nelson: Met. Trans., 1973, Vol. 4, pp. 364-366.
13. P. Kofstad: "High-Temperature Oxidation of Metals," John Wiley and Sons, Inc., New York, 1966.
14. A. D. McQuillan, Proc. Roy. Soc., 1950, A204, pp. 309-325.
15. T. A. Giorgi and F. Ricca, Nuovo Cimento Supp., 1967, Vol. 5, pp. 472-482.

16. G. Sanderson and J. C. Scully: Trans. AIME, 1967, Vol. 239, pp. 1883-1886.
17. C. J. Beevers, M. R. Warren, and D. V. Edmonds: J. Less-Common Met., 1968, Vol. 14, pp. 387-396.
18. R. I. Jaffee, G. A. Lenning, and C. M. Craighead: J. Metals, 1956, Vol. 8, pp. 907-913.
19. D. T. Powell and S. C. Scully: Corrosion, 1968, Vol. 24, p. 151.
20. G. G. Hancock and H. H. Johnson: Trans. AIME, 1966, Vol. 236, p. 513.
21. I. R. Lane, Jr., J. L. Cavallaro, and A. G. Morton: "Stress-Corrosion Cracking of Titanium." 1966, ASTM (Philadelphia), p. 246.
22. J. D. Boyd: Met. Trans., 1973, Vol. 4, pp. 1029-1035.
23. R. E. Curtis, R. R. Boyer, and J. C. Williams, Trans. ASM, 1969, Vol. 62, p. 457.
24. D. N. Fager and W. F. Spurr, Trans. ASM, 1968, Vol. 61, p. 283.
25. J. A. Feeney and M. J. Blackburn: Met. Trans., 1970, Vol. 1, pp. 3309-3323.
26. R. E. Curtis and W. F. Spurr, Trans. ASM, 1968, Vol. 61, p. 115.
27. J. C. Williams, N. E. Paton, P. J. Stocker, and H. L. Marcus: Proc. Nat. SAMPE Tech. Conf., 1971, pp. 643-650.
28. M. J. Blackburn and J. C. Williams: "Fundamental Aspects of Stress-Corrosion Cracking." 1969 (ed. R. W. Staehle), NACE (Houston), p. 620.
29. J. D. Boyd: Met. Trans., 1973, Vol. 4, pp. 1037-1045.
30. D. A. Meyn and G. Sandoz: Trans. AIME, 1969, Vol. 245, p. 1253.
31. J. C. Williams, R. R. Boyer, and M. J. Blackburn: "The Influence of Microstructure on the Fracture Topography of Titanium Alloys." 1968, Boeing Co., Document D6-23622, Renton, Washington.

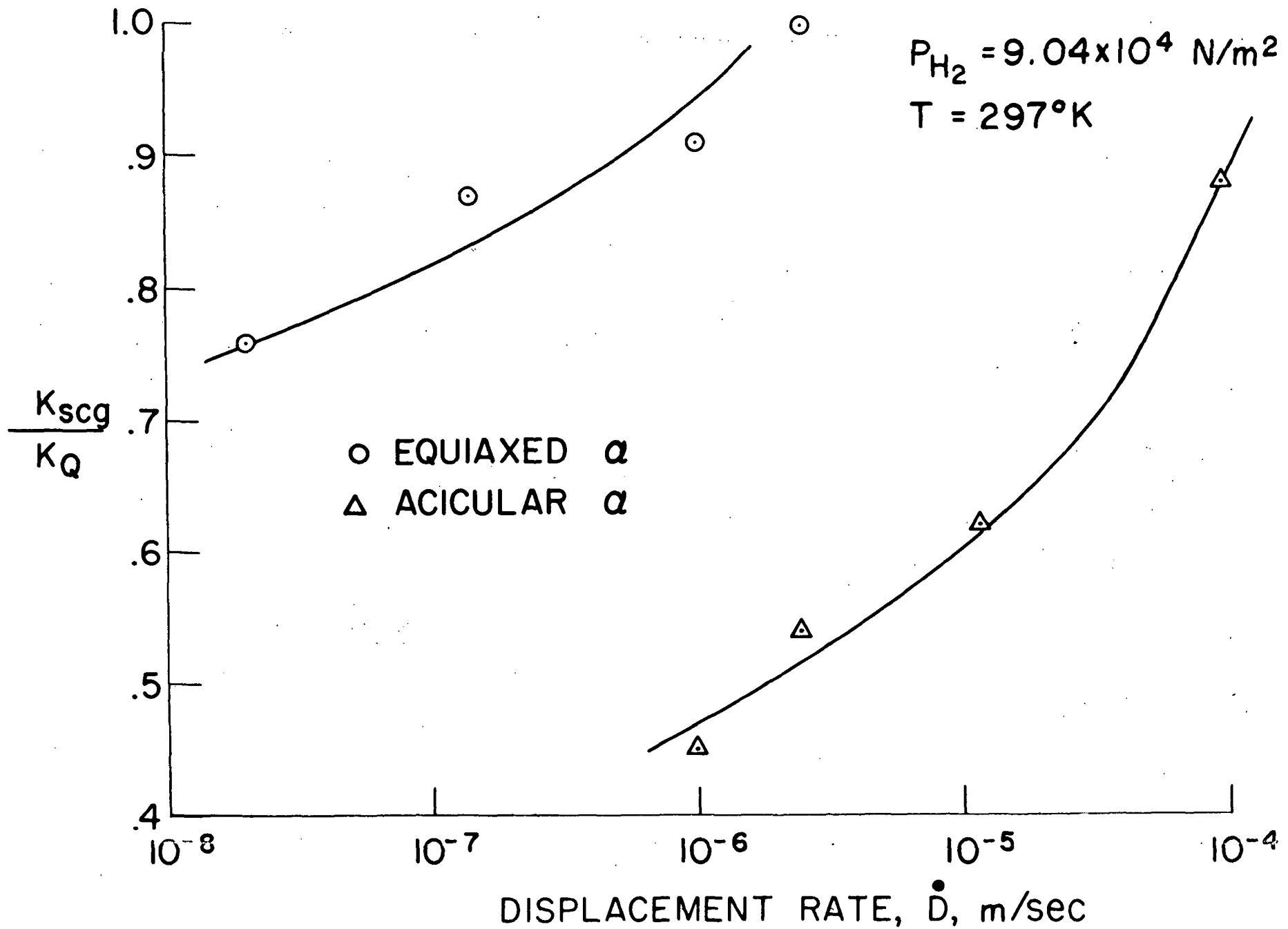


Fig. 1. - Gaseous hydrogen embrittlement of Ti-6Al-4V as a function of test displacement rate for two microstructures. (10)

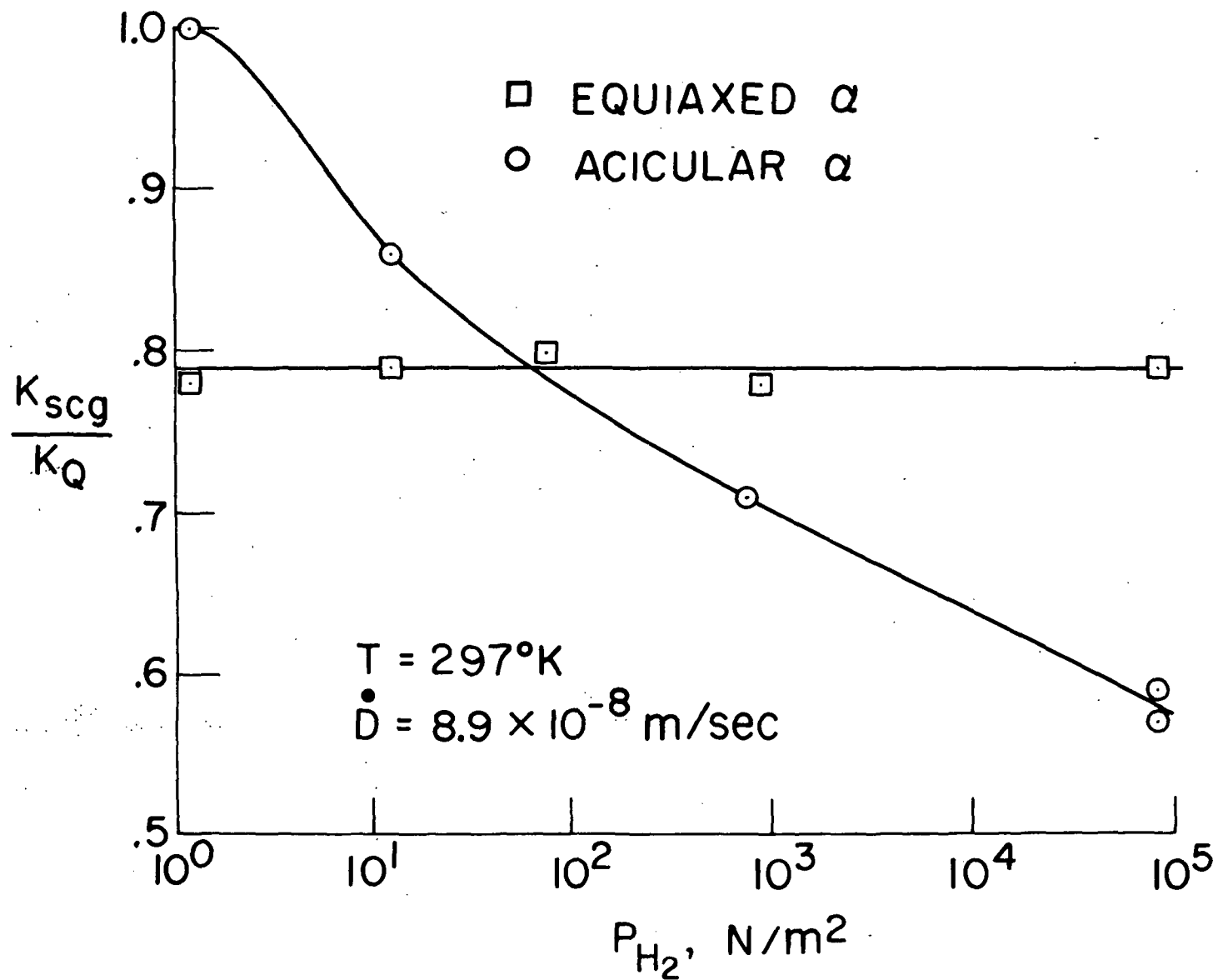
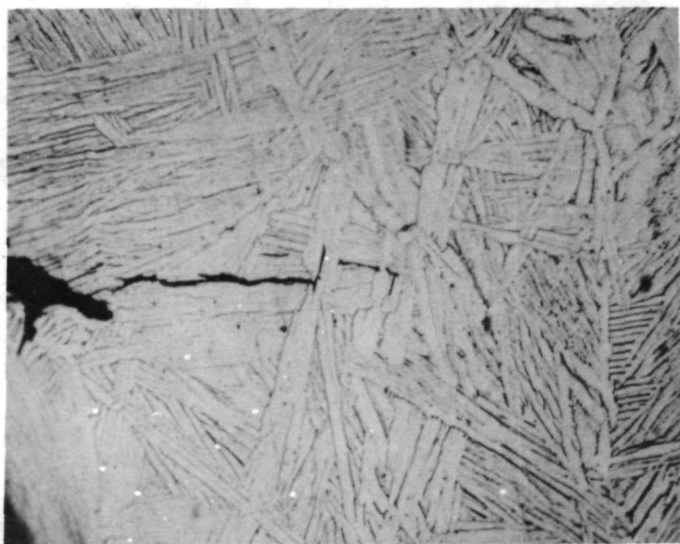
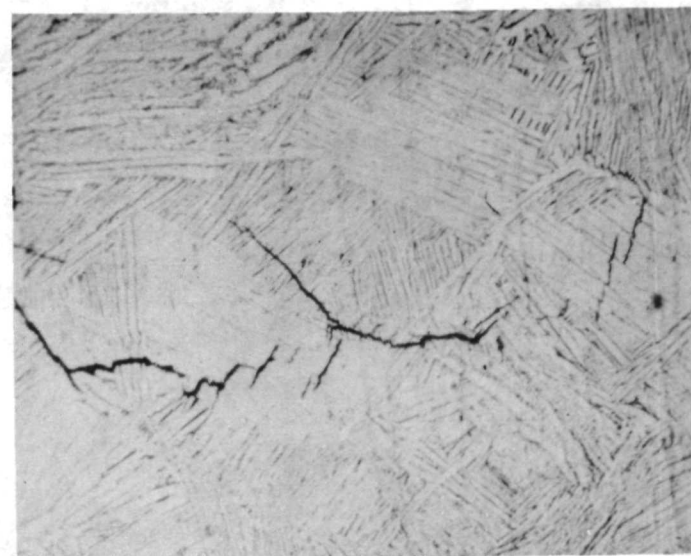


Fig. 2. - Gaseous hydrogen embrittlement of Ti-6Al-4V as a function of hydrogen pressure for two microstructures. (12)



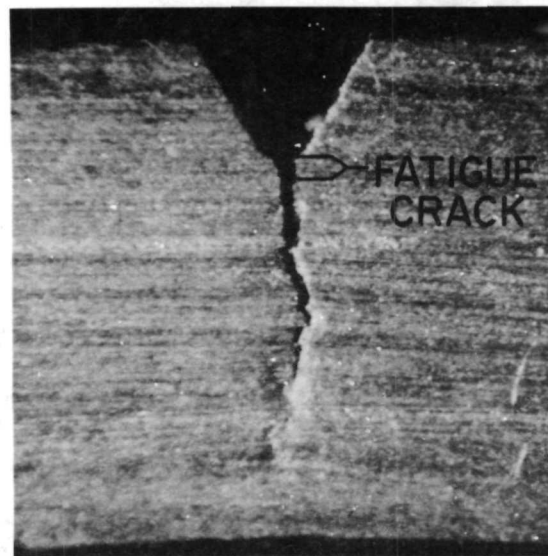
(a)

20 μ
└──┘

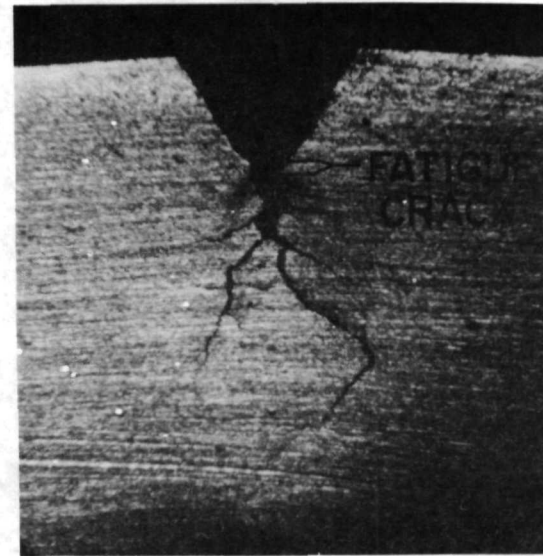


(b)

Fig. 3. - Microscopic hydrogen-induced cracking observed in Ti-6Al-4V specimens having an acicular α -phase microstructure tested at hydrogen pressures of (a) $9.06 \times 10^4 \text{ N/m}^2$ and (b) $1.3 \times 10^1 \text{ N/m}^2$.



(a)

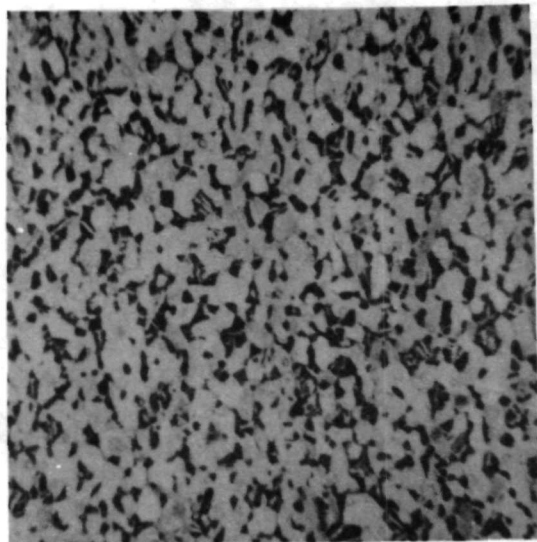


(b)

400 μ



Fig. 4. - Macroscopic hydrogen-induced cracking observed at a hydrogen pressure of 9.06×10^4 N/m² for Ti-6Al-4V specimens having (a) an acicular α -phase microstructure, and (b) equiaxed α -phase microstructure.



(a)

10 μ
└─┘



(b)

Fig. 5. - Representative microstructures of Ti-6Al-4V alloy given the following treatments: (a) solution treat at 1103°K for 40 min, water quench and 783°K age for 12 hr, and (b) solution treat at 1311°K for 40 min, stabilize at 977°K for 1 hr and 866°K for 1 hr, and air cool. Kroll's etch.

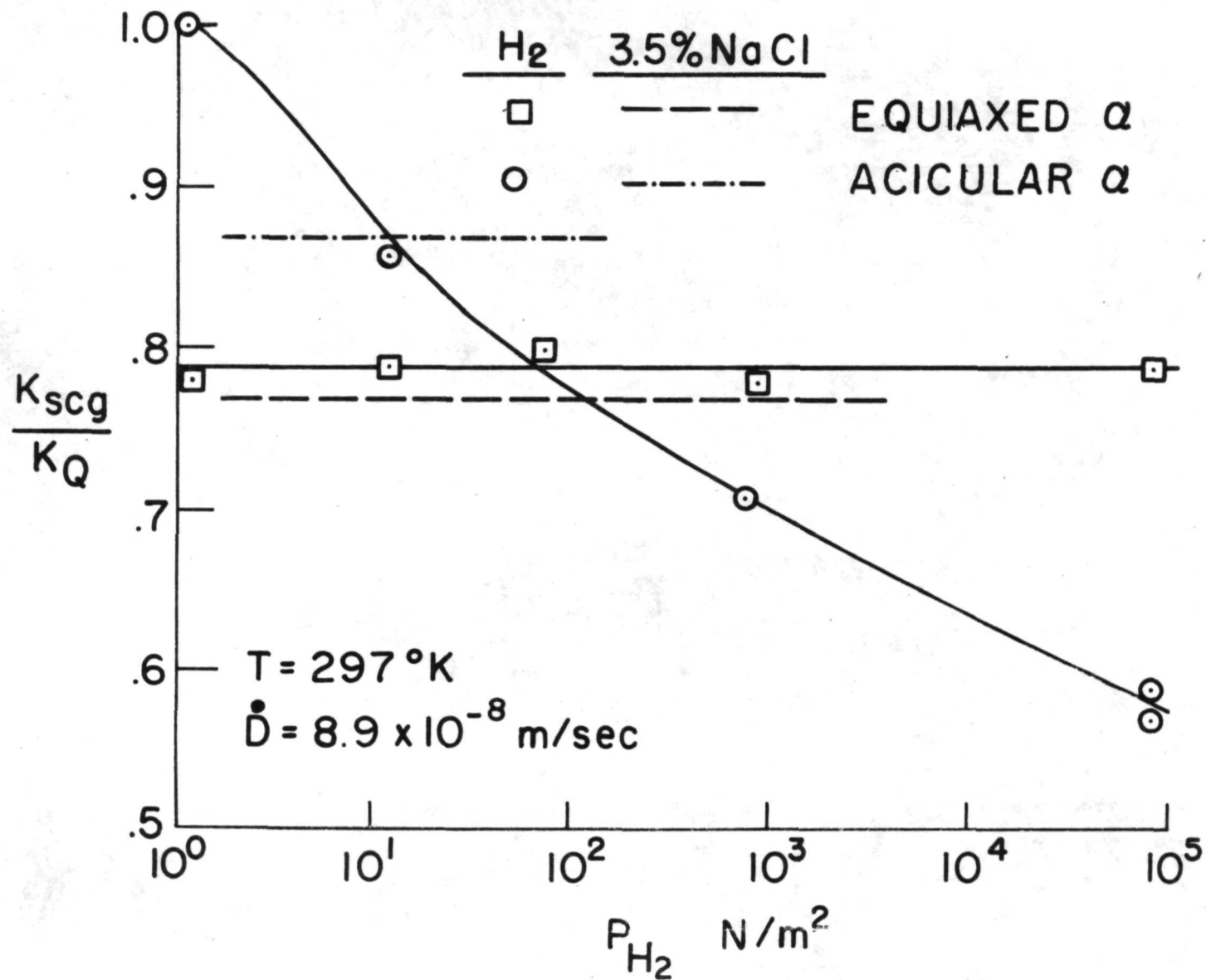
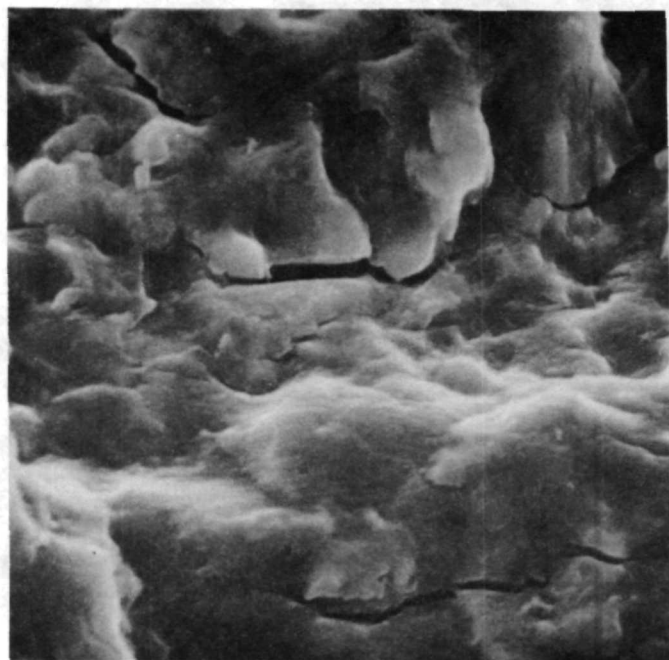
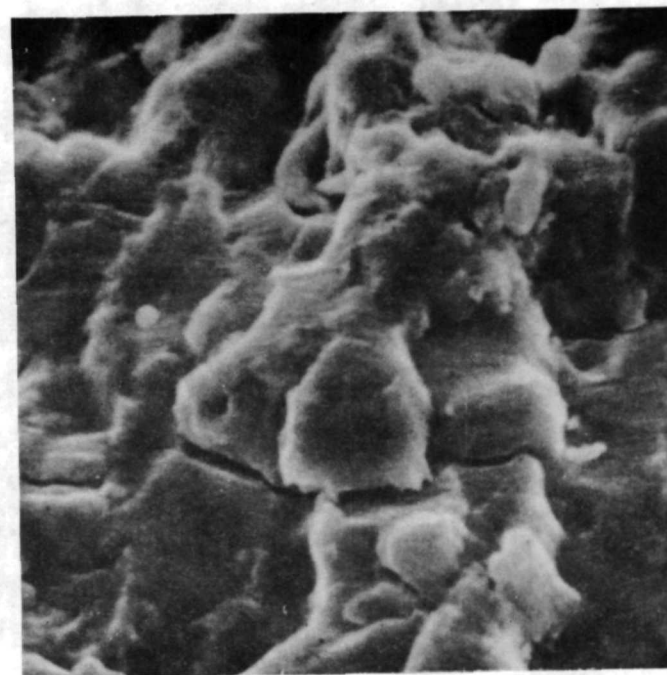


Fig. 6. - A comparison of severity of embrittlement observed in gaseous hydrogen as a function of hydrogen pressure⁽¹²⁾ and that observed in an aqueous chloride environment for two microstructures.



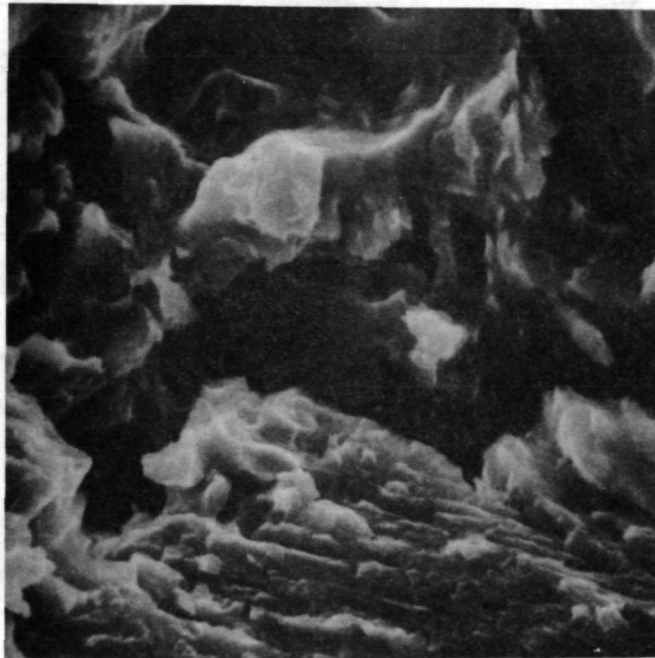
(a)



(b)

10 μ
└───┘

Fig. 7. - SEM fractographs of equiaxed specimens failed (a) in a gaseous hydrogen environment at 13 N/m² and (2) in an aqueous chloride environment.



10 μ
└──┘

Fig. 8. - SEM fractograph of an acicular specimen failed in an aqueous chloride environment.